Article

Analysis of Flow Characteristics and Effects of Turbulence Models for the Butterfly Valve

Sung-Woong Choi [1] [iD], **Hyoung-Seock Seo** [2] [iD] **and Han-Sang Kim** [3],*

1   Department of Mechanical System Engineering, Gyeongsang National University, 2, Tongyeonghaean-ro, Tongyeong-si 53064, Korea; younhulje@gmail.com
2   School of Naval Architecture and Ocean Engineering, University of Ulsan, Daehak-ro 93, Nam-gu, Ulsan 44610, Korea; seohs96@gmail.com
3   Department of Mechanical Engineering, Gachon University, 1342, Seongnam-daero, Sujeong-gu, Seongnam-si 13120, Korea
*   Correspondence: hahnsang@gmail.com

Abstract: In the present study, the flow characteristics of butterfly valves with different sizes DN 80 (nominal diameter: 76.2 mm), DN 262 (nominal diameter: 254 mm), DN 400 (nominal diameter: 406 mm) were numerically investigated under different valve opening percentages. Representative two-equation turbulence models of two-equation k-epsilon model of Launder and Sharma, two-equation k-omega model of Wilcox, and two-equation k-omega SST model of Menter were selected. Flow characteristics of butterfly valves were examined to determine turbulence model effects. It was determined that increasing turbulence effect could cause many discrepancies between turbulence models, especially in areas with large pressure drop and velocity increase. In addition, sensitivity analysis of flow properties was conducted to determine the effect of constants used in each turbulence model. It was observed that the most sensitive flow properties were turbulence dissipation rate (Epsilon) for the k-epsilon turbulence model and turbulence specific dissipation rate (Omega) for the k-omega turbulence model.

Keywords: butterfly valve; two-equation turbulence model; valve flow coefficient; sensitivity coefficient

1. Introduction

A valve is a device that regulates fluid flow by manipulating various passageways to control pressure and flow stream [1]. In the energy plant systems such as onshore and offshore plant systems, various sized valves are commonly used, where their sizes range from DN 6.35 (nominal diameter: 6.35 mm) for the small-sized to DN 1219 (nominal diameter: 1219 mm) for the large-sized to satisfy the operational requirements of a system, especially in the pipeline valves. Consideration of the engineering design for the sizes is important because selecting the correct sized valve requires knowledge of process conditions for valves in service [2]. The performance and characteristics of valves with different sizes can be determined and estimated with valve coefficients, such as flow coefficient, loss coefficient, and hydrodynamic torque coefficient; these standards have been widely published by Bosserman and American Water Works Association (AWWA) [3]. These valve characteristics are usually determined experimentally, however, it is sometimes not feasible to identify these factors [4] owing to limitations of experiments due to high cost and difficulty in experiments, especially for the large-sized. Therefore, numerical calculations can be usually applied to obtain valve coefficients.

To address these issues, several researchers have attempted to calculate valve coefficients numerically. Lin and Schohl [5] predicted the hydrodynamic force coefficients for a butterfly valve at different valve operating angles in an infinite flow field with numerical calculations. Song et al. [6] conducted a structural analysis of large butterfly valves using a numerical approach by validating three-dimensional (3D) experimental data of a butterfly

valve's pressure drop, flow coefficient, and hydrodynamic torque coefficient. Guan Song and Park [7] conducted three-dimensional numerical simulations for the butterfly valve to obtain valve flow coefficient and hydrodynamic torque coefficient used in a piping system. Henderson et al. [8] performed a numerical study of flow through a butterfly valve used in a hydroelectric power scheme. They predicted variations in hydrodynamic torque coefficient with the opening percentage of the disc during a constant head test with computational fluid dynamics (CFD) in a quasi-steady manner. Among lots of valve coefficients, especially for the valve flow coefficient, understanding of flow behavior with complicated flow configuration characteristics should be based, owing to the significance of the phenomena.

In the same manner, various investigations of flow behavior through valves have been conducted [9–12]. Huang and Kim [9] numerically analyzed the characteristics of butterfly valve flows with different disc angles for symmetric butterfly valves to simulate steady incompressible flow, and compared the numerical results with experiments carried out by Blevins [10]. Davis and Mike [11] predicted the flow coefficient of a globe valve using axisymmetric flow models with CFD analysis through 3D flows. Chern and Wang [12] studied flow behavior on a ball valve for the optimized control of ball valve performance by controlling the V-shaped opening of the valve in a pipe system.

Although the numerical predictions of flow behavior in the valve were greatly dependent on turbulence models, a few studies on turbulence model have been partly carried out by some researchers. Hinz et al. [13] presented normalized probability density functions of the filtered and unfiltered velocity increments with Navier–Stokes-$\alpha\beta$ regularization model at moderate Reynolds number (Re $\approx$ 200) in homogeneous isotropic turbulence. Thalabard et al. [14] conducted the study of the anomalous power-law to a general three-parametric class of the differential models relevant to several known examples of strong and weak finite capacity turbulence systems. Rigola et al. [15] carried out numerical studies focused on the numerical simulation model of the fluid flow through the valve reeds, considering a simplified geometry of an axial hole plus a radial diffuser.

In addition, numerical studies were conducted using CFD to analyze the turbulence model effect. Zhang et al. [16] conducted the studies for the two phases flow field numerical simulation inside the export ball valve of new rotor oil-gas mixture pump in different open height and different volume gas rate. With different conditions of the volume of gas rate, the velocity field and stress field in the ball valve were investigated. Leutwyler and Dalton [17] performed the numerical study for a compressible fluid flow through a butterfly valve, and the accuracy of different turbulence models was compared for the pressure profile. Said [18] investigated turbulence model effects on the accuracy of solutions for valve disc angles and implementation between experimental and numerical results. Most numerical studies on flow behavior through valves have been conducted without considering the effects of turbulence model, and the validity of the numerical results of the turbulence models remain uncertain. Therefore, in the present numerical study, the three turbulence models most frequently used were selected: two-equation $k - \varepsilon$ model of Launder and Sharma, two-equation $k - \omega$ model of Wilcox, and two-equation $k - \omega$ SST model of Menter. Limited studies on numerical approaches with turbulence models have been conducted, especially for the butterfly valve, although the range of their applications of the butterfly valve are increasing for various fluid dynamic systems and processes.

The present paper examined flow behavior and turbulence model effects on the flow behavior for different-sized butterfly valves with different disc opening percentage. The sensitivity analysis for the different two-equation turbulence models, $k - \varepsilon$ and $k - \omega$ model was conducted. The first part discusses a numerical study of flow behavior through different-sized butterfly valves under different disc openings of the valve. The effects of turbulence models of $k - \varepsilon$, $k - \omega$, and SST model on the flow characteristics were investigated. Sensitivity analysis of flow properties for the $k - \varepsilon$, $k - \omega$ turbulence models was performed in the second part to examine the effect of the turbulence model constant.

2. Theory

2.1. Turbulence Model

To determine the unknown Reynolds stress tensor, a transport equation was derived to develop a relationship between the Reynolds stress and known quantities of the mean flow. The Reynolds stress was modeled with Reynolds averaging process by an eddy viscosity model (EVM) to employ the Boussinesq hypothesis [19–22]. Reynolds stress can be expressed as follows:

$$\tau_{ij} = -\rho \overline{u}_i \overline{u}_j = \mu_t \left(\frac{\partial U_i}{\partial x_j} + \frac{\partial U_j}{\partial x_i} \right) - \frac{2}{3} \rho k \delta_{ij} \tag{1}$$

where k, ρ, δ_{ij}, τ_{ij} and μ_t represent the turbulent kinetic energy, density, Kronecker delta tensor, turbulence Reynolds stress, and eddy viscosity respectively. The velocity components and the mean velocity component in the x_i direction are denoted by u_i (i = 1, 2, 3) and capital U_i, respectively.

2.1.1. Two-Equation $k - \varepsilon$ Model of Launder and Sharma l

The $k - \varepsilon$ model (standard $k - \varepsilon$ model) is one of the most widely used two-equation eddy viscosity models incorporated in commercial CFD codes [23–26]. In this model, transport equations for turbulent kinetic energy (k) and dissipation rate (ε) are expressed as

$$\frac{\partial(\rho k)}{\partial t} + \frac{\partial}{\partial x_j} \left(\rho u_j \frac{\partial k}{\partial x_j} - \left(\mu + \frac{\mu_t}{\sigma_k} \right) \frac{\partial k}{\partial x_j} \right) = \tau_{ij} S_{ij} - \rho \varepsilon + \text{\OE}_k \tag{2}$$

$$\frac{\partial(\rho \varepsilon)}{\partial t} + \frac{\partial}{\partial x_j} \left(\rho u_j \varepsilon - \left(\mu + \frac{\mu_t}{\sigma_\varepsilon} \right) \frac{\partial \varepsilon}{\partial x_j} \right) = C_{1\varepsilon} \frac{\varepsilon}{k} \tau_{ij} S_{ij} - C_{2\varepsilon} f_2 \rho \frac{\varepsilon^2}{k} + \text{\OE}_\varepsilon \tag{3}$$

The turbulence constants typically used in the model were five empirical constants: C_μ, $C_{1\varepsilon}$, $C_{2\varepsilon}$, σ_k and σ_ε. The near wall damping functions and the explicit wall terms are expressed as follows:

$$f_\mu = \exp(-3.4/(1 + 0.02\text{Re}_t)^2), \ f_2 = 1 - 0.3\exp(-\text{Re}_t{}^2), \text{Re}_t = \frac{\rho k^2}{\varepsilon \mu}$$

$$\phi_k = 2\mu \left(\frac{\partial \sqrt{k}}{\partial y} \right)^2 \text{ and } \phi_\varepsilon = 2\mu \frac{\mu_t}{\rho} \left(\frac{\partial^2 u_s}{\partial y^2} \right)^2,$$

where u_s is the flow velocity parallel to the wall.

The turbulence constants used in the $k - \varepsilon$ model have been described by Bottema [27], Comte-Bellot and Corrsin [28], Hrenya et al. [29], Launder and Spalding [30,31], and Shih [32]; the most frequently used are the following constants: $C_{\varepsilon 1}$, $C_{\varepsilon 2}$, C_μ, σ_k and σ_ε as 1.44, 1.92, 0.0900, 1.00, and 1.30, respectively [33]. However, the range of constant values was seen to be wide range of values: values for $C_{\varepsilon 1}$, $C_{\varepsilon 2}$, C_μ, σ_k and σ_ε range between (1.15:1.50) [29,33–35], (1.68:2.00) [35,36], (0.0300:0.0900) [27,32], (0.500:1.75) [31], (0.610:1.36) [27], respectively [37].

2.1.2. Two-Equation $k - \omega$ Model of Wilcox

In this model, convective transport equations are solved for the turbulent kinetic energy, k and its specific dissipation rate, ω. The eddy viscosity is defined as the function of relationship between turbulence kinetic energy and the specific dissipation rate, represented by the ratio of dissipation and turbulence intensity from Kalitzin et al. [38], which was developed by Wilcox [23,39] as follows:

$$\mu_t = \rho \frac{k}{\omega} \tag{4}$$

Two transport equations are composed of two-equation expressed with the turbulence kinetic energy, k and specific dissipation rate, ω, as the following:

$$\frac{\partial(\rho k)}{\partial t} + \frac{\partial}{\partial x_j}\left(\rho u_j k - \left(\mu + \frac{\mu_t}{\sigma_k}\right)\frac{\partial k}{\partial x_j}\right) = \tau_{ij}S_{ij} - \beta'\rho k\omega \tag{5}$$

$$\frac{\partial(\rho\omega)}{\partial t} + \frac{\partial}{\partial x_j}\left(\rho u_j \omega - \left(\mu + \frac{\mu_t}{\sigma_\omega}\right)\frac{\partial\omega}{\partial x_j}\right) = \alpha\frac{\omega}{k}\tau_{ij}S_{ij} - \beta\rho\omega^2 \tag{6}$$

The turbulence constants mostly frequently used in the model were five empirical constants with the following values [23,39]: $\alpha = 0.556$, $\beta = 0.0750$, $\beta' = 0.090$, $\sigma_k = 2$, $\sigma_\omega = 2$. However, the constants used in the model were also a wide range of values: values for α, β, β', σ_k and σ_ω range between (0.52:0.556) [39], (0.075:0.083) [40], 0.09 [23,36], (1.5:2) [41], (1.67:2) [39,41], respectively.

2.1.3. Shear Stress Transport (SST) Model

In the SST model, the eddy viscosity is expressed with the function of the turbulence kinetic energy and the specific dissipation rate as follows [40]:

$$\mu_t = \rho\frac{k/\omega}{\max(1; \Omega F_2/a_d\omega)} \tag{7}$$

The eddy viscosity value was influenced by the specific dissipation rate and a_l. The specific dissipation rate can be obtained with an auxiliary function. The auxiliary function is defined as a function of wall distance of d as follows [40]:

$$F_2 = \tan\left\{\left(\max\left[2\frac{\sqrt{k}}{0.09\omega d}; \frac{500\mu}{\rho d^2\omega}\right]\right)^2\right\} \tag{8}$$

Two transport equations for the SST model can be defined with a blending function of F_1 for the model coefficients of turbulence dissipation rate, ε and specific dissipation rate, ω. The transport equation for the turbulent kinetic energy is expressed, as the following [42]:

$$\frac{\partial(\rho k)}{\partial t} + \frac{\partial}{\partial x_j}\left(\rho u_j k - \left(\mu + \frac{\mu_t}{\sigma_k}\right)\frac{\partial k}{\partial x_j}\right) = \tau_{ij}S_{ij} - \beta'\rho k\omega \tag{9}$$

$$\frac{\partial(\rho\omega)}{\partial t} + \frac{\partial}{\partial x_j}\left(\rho u_j \omega - \left(\mu + \frac{\mu_t}{\sigma_\omega}\right)\frac{\partial\omega}{\partial x_j}\right) = P_\omega - \beta\rho\omega^2 + 2(1 - F_1)\frac{\rho\omega_{\omega 2}}{\omega}\frac{\partial k}{\partial x_j}\frac{\partial\omega}{\partial x_j} \tag{10}$$

where P_ω is the production term of ω which can be expressed with vorticity as follows:

$$P_\omega \equiv 2\gamma\rho\left(S_{ij} - \frac{\omega S_{nn}\delta_{ij}}{3}\right)S_{ij} = \gamma\rho\Omega^2 \tag{11}$$

The blending function F_1 expressed formally can be defined as

$$F_1 = \tanh\left\{\left(\min\left[\max\left[\frac{\sqrt{k}}{0.09\omega d}; \frac{500\mu}{\rho d^2\omega}\right]; \frac{4\rho\sigma_{\omega 2}k}{CD_{k\omega}d^2}\right]\right)^4\right\} \tag{12}$$

where $CD_{k\omega}$ is cross-diffusion term in the $k - \varepsilon$ model as follows:

$$CD_{k\omega} = \max\left[\frac{2\rho\sigma_{\omega 2}}{\omega}\frac{\partial k}{\partial x_j}\frac{\partial\omega}{\partial x_j}; 10^{-20}\right] \tag{13}$$

The turbulence constants in this model expressed with the combination of symbol φ defined by blending the coefficients in the $k - \omega$ model and $k - \varepsilon$ model, denoted as φ_1 and φ_2, respectively [43], as follows:

$$\varphi = F_1\varphi_1 + (1 - F_1)\varphi_2, \ \varphi = \{\sigma_k, \sigma_\omega, \beta, \gamma\} \tag{14}$$

2.2. Flow Coefficient of a Valve

A valve flow coefficient, C_v, is one of the practical methods to determine the size of the valve, which was first introduced by Masoneilan in 1944 [44]. According to the ISA standard S75.01, 02 [45,46], a valve flow coefficient is defined as the quantity of water in US gallons at 60 °F that passes through the valve under a pressure drop of 1 psi [44–46]. The measurement of the valve flow coefficient given by the ISA standard S75.01, 02 [45,46] for incompressible, fully turbulent, non-cavitation, and non-flashing flow is written as

$$C_v = \frac{Q}{N_1}\sqrt{\frac{G_f}{\Delta p}} \tag{15}$$

where Q, N_1, G_f, and Δp is the volumetric flow rate, constant used in the valve flow coefficient, specific gravity of the fluid, and pressure difference between upstream and downstream location, respectively [45,46]. The valve flow coefficient with the opening percentage of the valve disc is known as the indicator of how flow rate will change with an opening percentage [47].

3. Numerical Implementation

In the numerical formulations for the present study, different-sized butterfly valves were considered, and the experimental data on flow coefficients for valve sizes DN 80 (76.2 mm), DN 262 (254 mm), and DN 400 (406 mm) were obtained from the previous studies performed by Sandalci et al. [48], Nazary et al. [49], and Kim et al. [50]. Numerical studies were carried out with the same conditions used in the experiments for comparison with experimental results. The governing equations for turbulent flow consisted of mass and momentum conservation equation along with different two-equation turbulence models of $k - \varepsilon$, $k - \omega$, and SST to predict the Reynolds stresses. The governing equations with the boundary conditions were solved using the finite volume method in the commercial CFD package ANSYS-CFX (ANSYS, version 14.5).

3.1. Calculation Conditions

The three different sizes of butterfly valves were modeled with different opening percentages of disc from 10% to 100%, for the disc modeling with solid body. The illustrations of calculation domain are shown in Figure 1. According to research by Kim [9], the distance from the valve required for the flow to fully develop upstream and downstream lengths was determined to be five and 10 times the valve size. The flow characteristics around the butterfly valve were investigated with water as the working fluid with a density of 999 kg/m^3 and dynamic viscosity of 1.12×10^{-3} N·S/m^2. The constant used in the valve flow coefficient was adopted according to the ISA standard [45,46]. The flow was assumed to be incompressible and steady. The pressure difference and corresponding flow rates were used to calculate the valve flow coefficient using Equation (15). The pressure difference between the inlet and outlet boundary conditions were set at uniform pressure of 1 bar to satisfy the valve flow coefficient conditions. With regard to the constants for the two-equation turbulence models of $k - \varepsilon$, $k - \omega$, and SST, the nominal values are used as following: $C_{\varepsilon 1} = 1.44$, $C_{\varepsilon 2} = 1.92$, $C_\mu = 0.09$, $\sigma_k = 1.00$, $\sigma_\varepsilon = 1.30$ for the $k - \varepsilon$ model, $\alpha = 0.556$, $\beta = 0.075$, $\beta' = 0.090$, $\sigma_k = 2.00$, $\sigma_\omega = 2.00$ for the $k - \omega$ model, respectively. The scalable wall function and automatic wall function approach was applied. A structured and non-adaptive grid (hexahedral grid) was generated. For the pipe wall, a no-slip boundary condition was applied. The turbulence intensity was set to 5~10% at the inlet [23]. For the near wall flow model, a maximum value of 20 for y+ was considered close to the valve sur-

face and pipe wall, based on the research by Launder and Spalding [31]. A high-resolution advection scheme was used and a convergence criterion for maximum root-mean-square residual of 10^{-6} was set, which is two orders of magnitude below the default convergence level of the solver [8,51].
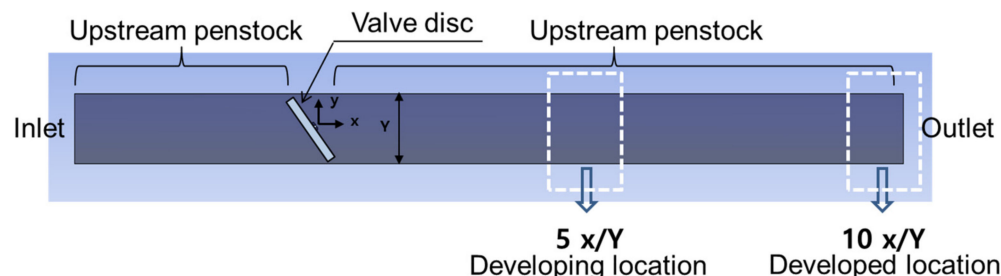

Figure 1. Illustrations of calculation region for the cross section of a single butterfly valve.

3.2. Mesh Dependence Study

The mesh size dependence study was performed with numerical calculation of the flow coefficient by means of Equation (15), for the representative DN 80 butterfly valve with 50% opening percentage with respect to turbulence models by successively decreasing the element size with a structured grid—a coarse grid with 250,000 meshes; a medium grid with 350,000 and 390,000 meshes; and a fine grid with 450,000 meshes. The number of mesh elements was increased gradually until the solution becomes independent of the mesh density while avoiding skewness and aspect ratio violations [52]. The results are listed in Figure 2. The resulting variations in the solution decreased with decreasing the element size and the results obtained for cell resolution of approximately 400,000 were selected in the present study. In the same manner, mesh element was chosen, 380,000 and 360,000 for the DN 262 and DN 400, respectively.
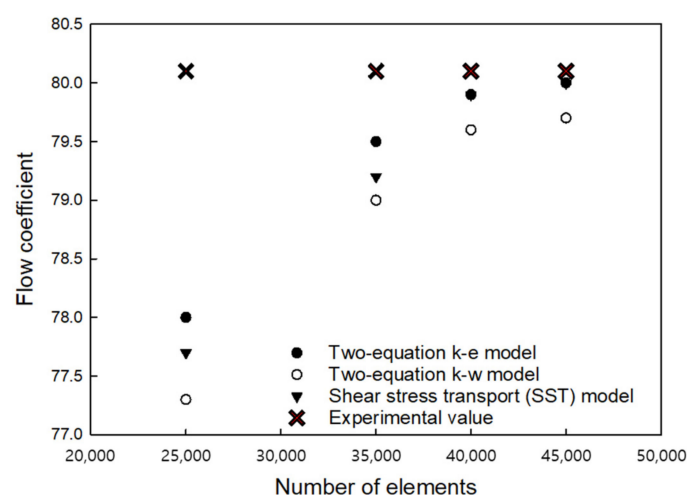

Figure 2. Result of mesh size dependence study for flow coefficient.

4. Results and Discussion

4.1. Flow Coefficient

A numerical approach for the flow behavior through the valve was validated by comparison with the experimentally measured flow coefficient, and the effect of the turbulence models with nominal value of turbulence constants was estimated by comparison of the flow coefficients between numerical and experimental results. The discrepancies of flow coefficient results of the different-sized valves with different turbulence models are shown in Figure 3. Regarding the discrepancies between numerical and experimental results for flow coefficients for the different valve sizes, it is shown that the discrepancy increased

with increasing valve size, and different degrees of discrepancy were observed with percentage of disc opening for each valve size. For DN 80, numerical results were within 5% discrepancy with turbulence models, and the discrepancy increased with the percentage of disc opening. For DN 262, the discrepancy was within 8%, especially with disc opening over 80%. For DN 400, within 10% discrepancy was observed with disc opening over 70%. The results in Figure 3 show that discrepancies varied with valve size, indicating that specific turbulence model did not satisfy numerical predictions for all valve sizes. For the case of DN 80 and DN 262, the $k - \omega$ and SST models were suitable except for the 40–70% disc opening. For the case of DN 400, the $k - \omega$ and SST models were suitable for all disc openings except for the 60–90% disc opening, for which the $k - \varepsilon$ model was suitable.
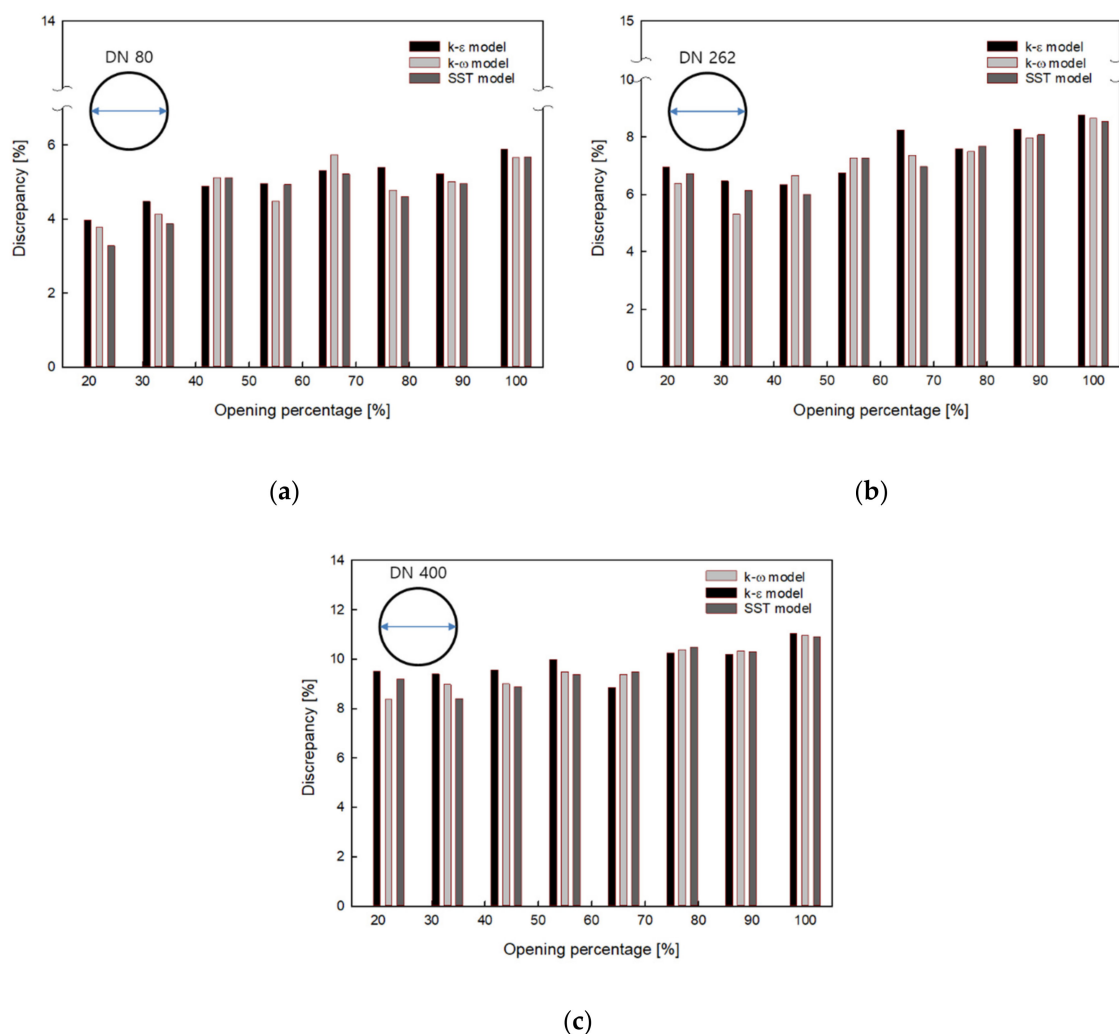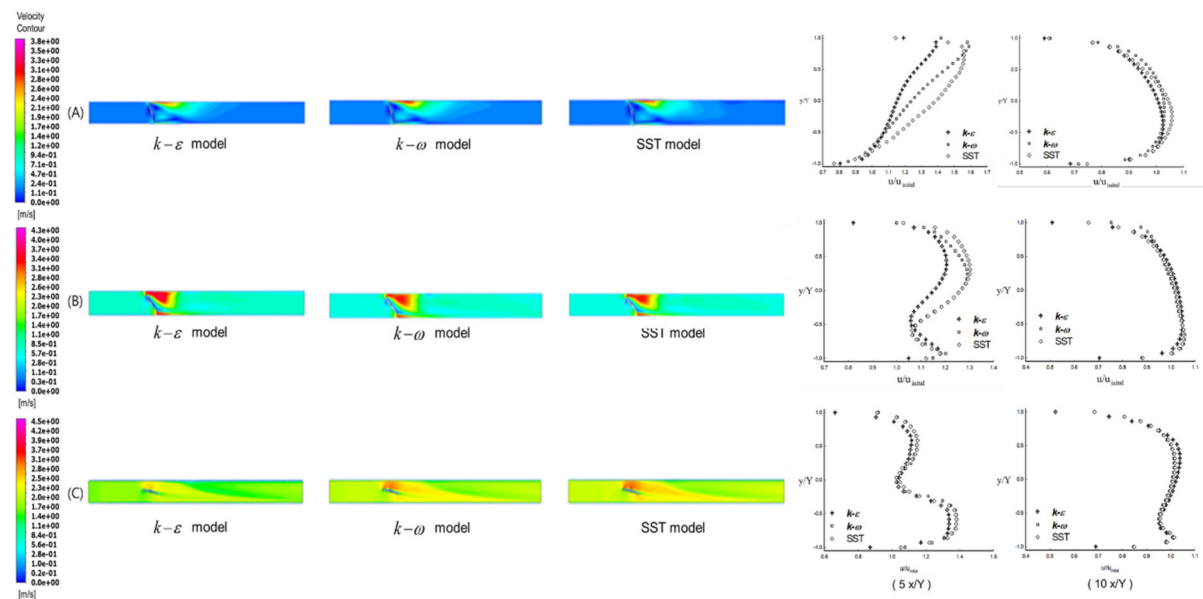

(a)

(b)

(c)

Figure 3. Discrepancies of flow coefficient results for the different turbulence models with different-sized valves and opening percentage: (**a**) DN 80 valves, (**b**) DN 262 valves, (**c**) DN 400 valves.
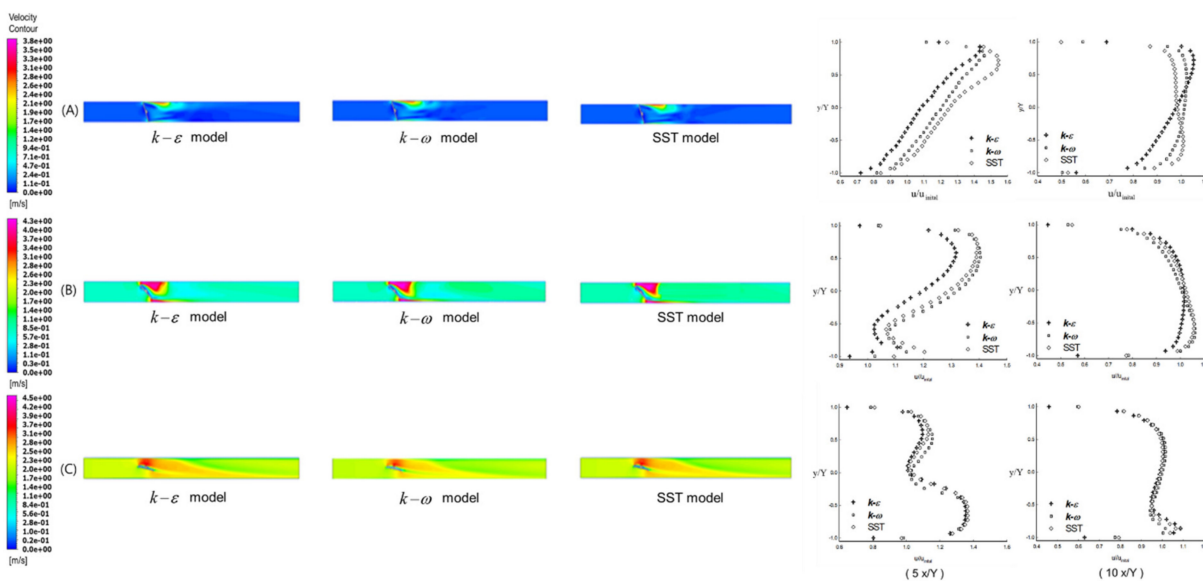
4.2. Flow Behavior

Figure 4 shows the velocity contour and profile for the DN 80, DN 262, and DN 400 valves under different disc opening percentages with two-equation $k - \varepsilon$, $k - \omega$, and SST turbulence models. The flow behavior and turbulence characteristics were observed with velocity profiles in two characteristic locations: 5 x/Y and 10 x/Y with the developing and the developed flow region, respectively, where x is the distance from the valve and Y is the nominal valve size. Velocity profile was presented with the ratio of velocity of cross section to the initial velocity at two characteristic locations. The fully developed region,

development length was shown for the effective flow region. Flow analysis was conducted with different valve disc configuration in CFD model for each case.
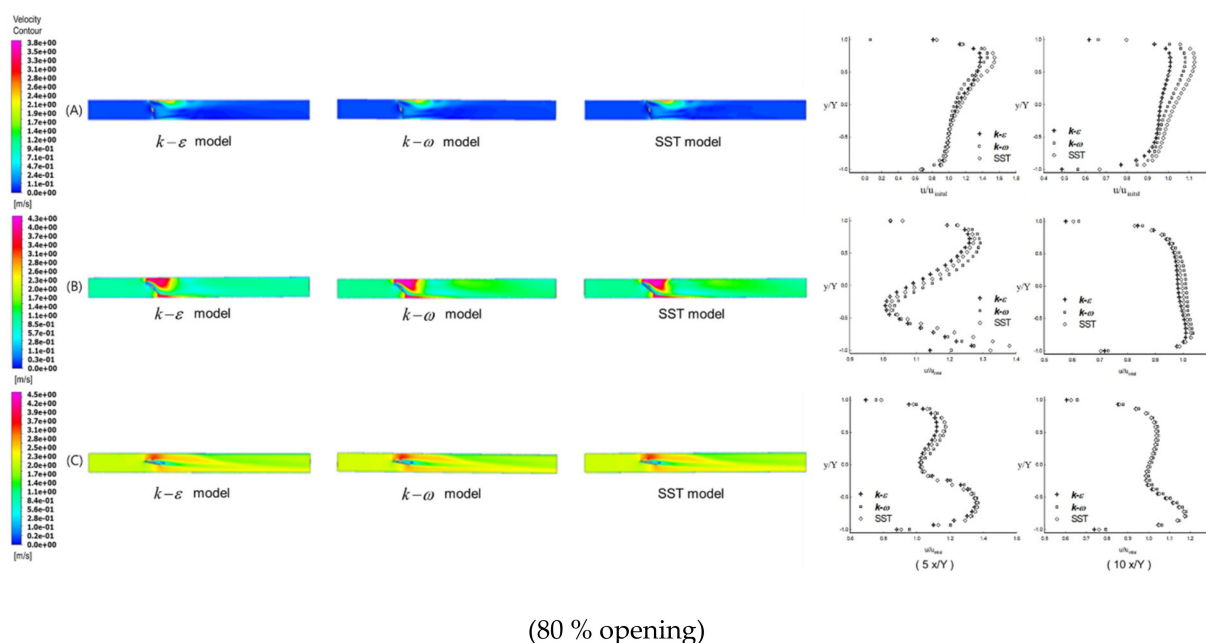

(20 % opening)

(50 % opening)

Figure 4. *Cont.*

(80 % opening)

Figure 4. Velocity contour and profile with different opening for the $k - \varepsilon$, $k - \omega$, and SST turbulence models: (**A**) DN 80, (**B**) DN 262, (**C**) DN 400.

For the small disc opening of 20% at location 5 x/Y, wake region containing vortices induced were generated from the upper side direction behind the valve disc owing to the high disturbance of the flow. The higher turbulence owing to vortices was observed for the $k - \omega$ model expressed with higher turbulence kinetic energy as shown in Figure 5. With flow passing through the gap between the disc and pipe wall, the increased reattachment point toward the downstream direction for the $k - \omega$ model was observed. Flow mixing with vortices is seen to be developed with wake and recirculation regions for the SST model. Meanwhile, smaller turbulence kinetic energy and wake region were expressed by the $k - \varepsilon$ model. With increasing valve size in the case of DN 400, the tendency that less velocity changes through the valve disc was expressed with smaller vortex regions in the stream-wise direction, compared to larger changes in the case of the DN 80 valve. With developed flow at location 10 x/Y, each flow passing through the gap was mixed. With increasing valve size, flow mixing was seen to develop in the upper side. This is due to relatively larger flow in the gap between the disc and wall of the valve.
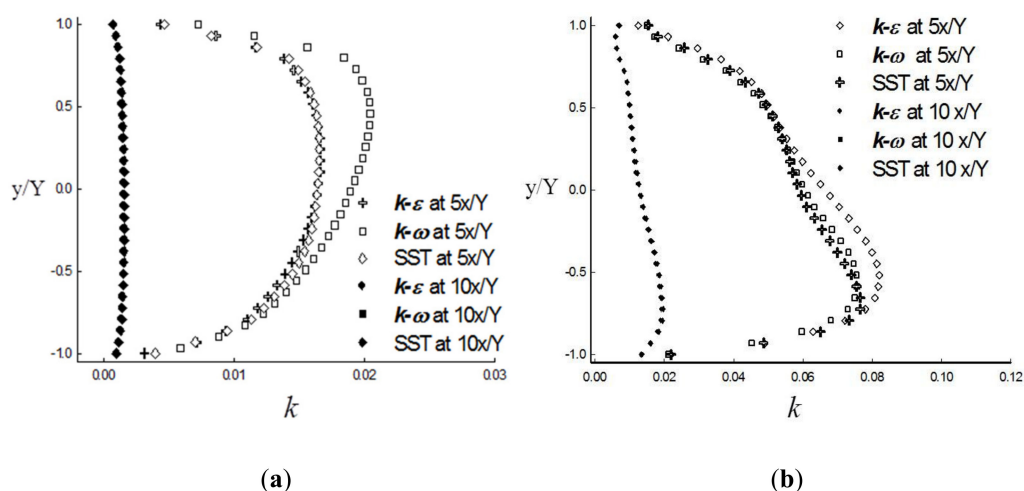

Figure 5. Turbulence kinetic energy profile with 20% opening for the DN 80 (**a**) and 50% opening for the DN 262 (**b**), with different turbulence model of $k - \varepsilon$, $k - \omega$ and SST.

At 50% disc opening percentage as shown in Figure 4, flow recirculation and secondary flow developed near the valve disc in the form of vortex mixing. With increasing opening percentage, larger flow passing through the gap between the disc and pipe wall resulted in a circulation region that moved closer to the disc. Henderson et al. [8] and Del Toro [4] reported similar results for turbulent and vortex behavior. At location 5 x/Y, flow disturbances due to vortices were expressed by the $k - \omega$ model, representing higher turbulence kinetic energy, followed by the SST and $k - \varepsilon$ models for the DN 80 valve. At location 10 x/Y, the velocity profile was shown to be twisted toward the downstream direction. Flow disturbance, mixing, and secondary flow due to vortices were seen to develop for the $k - \omega$ model, and followed by SST model. At location 10 x/Y, as valve size increased, the twisted velocity profile changed more uniformly in cross section, and there was little change in velocity profile between the turbulence models.

With large opening of 80% as shown in Figure 4, due to the large flow area between the disc and the pipe wall, the amount of recirculation and vortex behind the valve disc was reduced. Two stream-wise secondary flows were developed and separated after passing through the valve disc. Vortex regions were rapidly dissipated along the downstream due to large currents. The secondary flow developed close to the valve disc made the downstream flow considerably smoother. The two secondary flows flowing along both sides of the valve disc mixed and developed with a vortex in the downstream direction. A vortex region with eddies behind the valve disc was observed as valve size increased to the DN 400 valve.

In sum, among the turbulence models, the largest pressure drop was observed in $k - \varepsilon$ turbulence models showing higher turbulence kinetic energy in Figure 5. Large pressure drops had an effect on the estimation of flow coefficient, C_v, with large value. On the other hand, relatively smaller pressure drop can be obtained in $k - \omega$, and SST turbulence models. This effect of turbulence model can be attributed to the amount of discrepancy with turbulence models, therefore, the largest discrepancy between calculation and experimental value for the flow coefficient can be observed in $k - \varepsilon$ turbulence models, which is mentioned in Section 4.1. Furthermore, the overall comparison between turbulence models yielded the value of differences: the difference between turbulence models increased with decreasing valve size and disc opening percentage. As the valve size and disc opening decrease, a smaller flow region with a relatively small area between the disc and the valve wall caused a large pressure drop, which increases the turbulence as seen in the increasing behavior of turbulent kinetic energy. Therefore, among two-equation turbulence model, priority should be given to $k - \omega$, and SST turbulence models. This is especially considered for the design of valve facilities that are relatively small sized and have large pressure drops.

5. Sensitivity Analysis

According to the assumption of the two-equation method of $k - \varepsilon$ model and $k - \omega$ model, the time-averaged values based on the simplified assumptions: Reynolds averaging, Boussinesq approximation, Prandtl hypotheses, etc. [53] These time-averaged assumptions require turbulence model constants to account for turbulence, therefore, in this study, the effects of turbulence model constants should be assessed by the sensitivity study. For the present sensitivity study, the methods developed by the Błazik-Borowa [37,54] and the group of Pelletier [55] were adopted. The main flow properties based on the time-averaged values were described as follows: the stream-wise flow-velocity (u), turbulence kinetic energy (k), turbulence dissipation rate (ε), turbulent eddy viscosity (μ_t) for the two-equation of $k - \varepsilon$ turbulence model, and stream-wise flow-velocity (u), turbulence kinetic energy (k), turbulence specific dissipation rate (ω), turbulent eddy viscosity (μ_t) for the two-equation of $k - \omega$ turbulence model. The sensitivity of the flow properties to the constants for

each turbulence model was examined with sensitivity coefficients using finite difference approximations taking the following form [37,54]:

$$\widetilde{S}_m = \frac{w_2 - w_1}{\Delta C_m} \tag{16}$$

where $\widetilde{S}_m$, ΔC_m, w_1 and w_2 are the sensitivity coefficient, increment of examined constants, and calculation results at $C_m - \Delta C_m/2$ and $C_m + \Delta C_m/2$, respectively.

For the case of the DN 80 valve, sensitivity analyses were conducted using Equation (16) under different opening percentage conditions. For the flow properties, the examined constants for the each turbulence model are as follows: $C_{\varepsilon 1}$, $C_{\varepsilon 2}$, C_μ, σ_k, σ_ε for the $k - \varepsilon$ model, and α, β, β', σ_k, σ_ω for the $k - \omega$ model. Increment of examined constants for the sensitivity analysis with turbulence model is as follows: $\Delta C_{\varepsilon 1}$, $\Delta C_{\varepsilon 2}$, $\Delta \sigma_k$, $\Delta \sigma_\varepsilon$ are 0.1 and ΔC_μ is 0.01 [37,54] for the $k - \varepsilon$ model, and $\Delta \alpha$, $\Delta \beta$, $\Delta \beta'$, $\Delta \sigma_k$, $\Delta \sigma_\omega$ are 0.01 for the $k - \omega$ model.

5.1. Sensitivity Result of Two-Equation $k - \varepsilon$ Model

Figure 6 presents the extreme values of sensitivity coefficients with respect to the constants for the $k - \varepsilon$ turbulence model. The flow properties were obtained at the 5 x/Y, developing region and 10 x/Y, developed region. Individual sensitivity coefficients had different shapes for individual flow properties, and varied with disc opening cases. The resulting sensitivity coefficients had both positive and negative values, where positive values mean increasing functions of the constant and negative values mean decreasing functions [37,54].
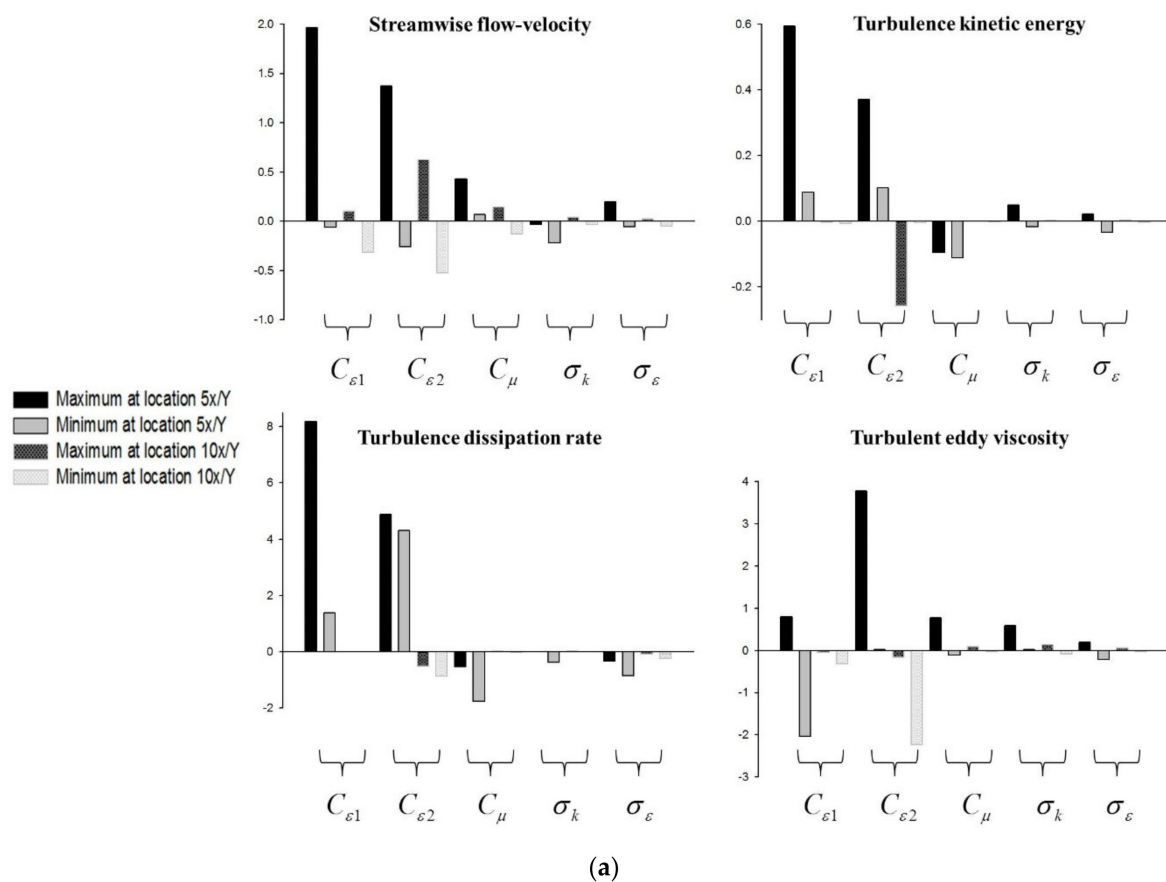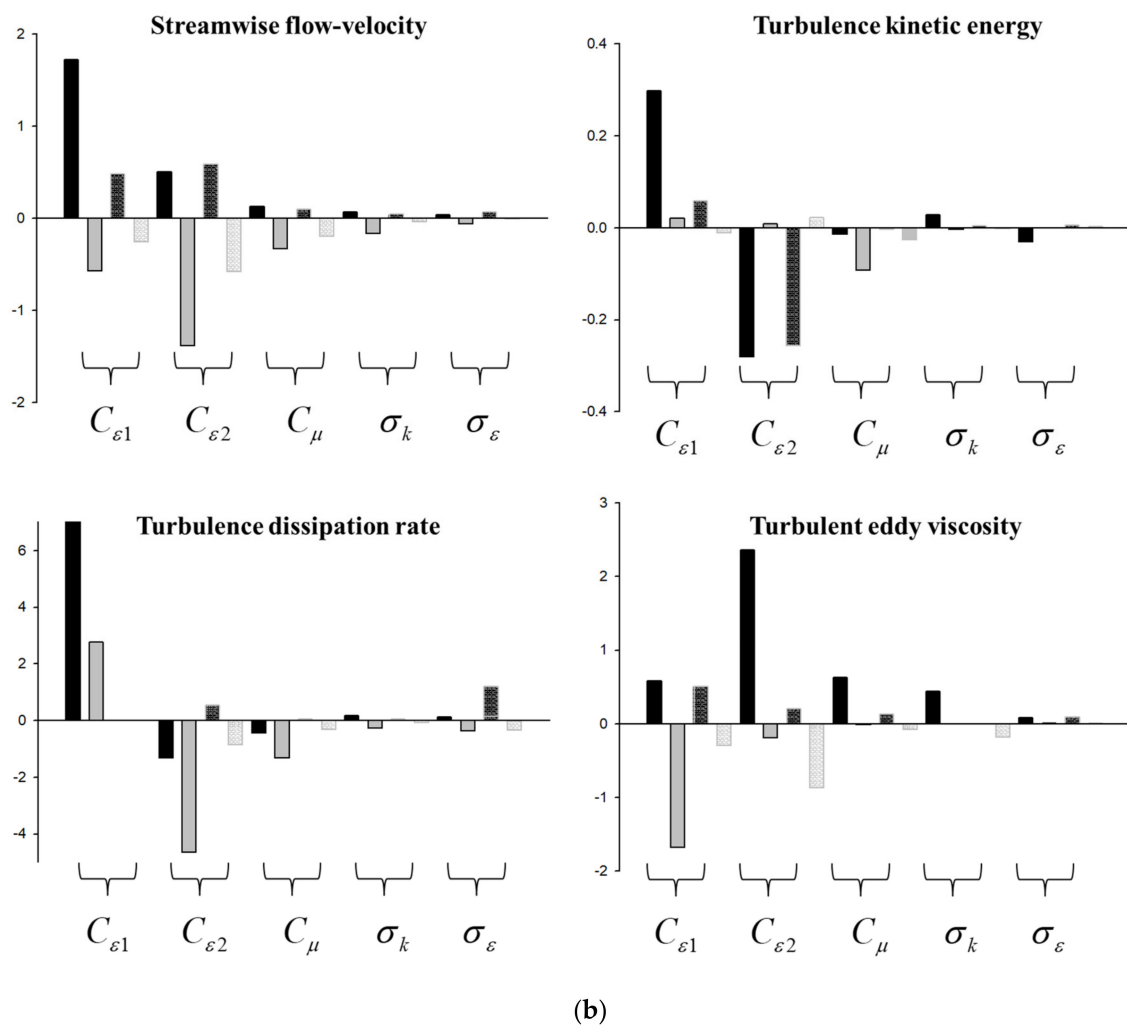

(**a**)

Figure 6. *Cont.*
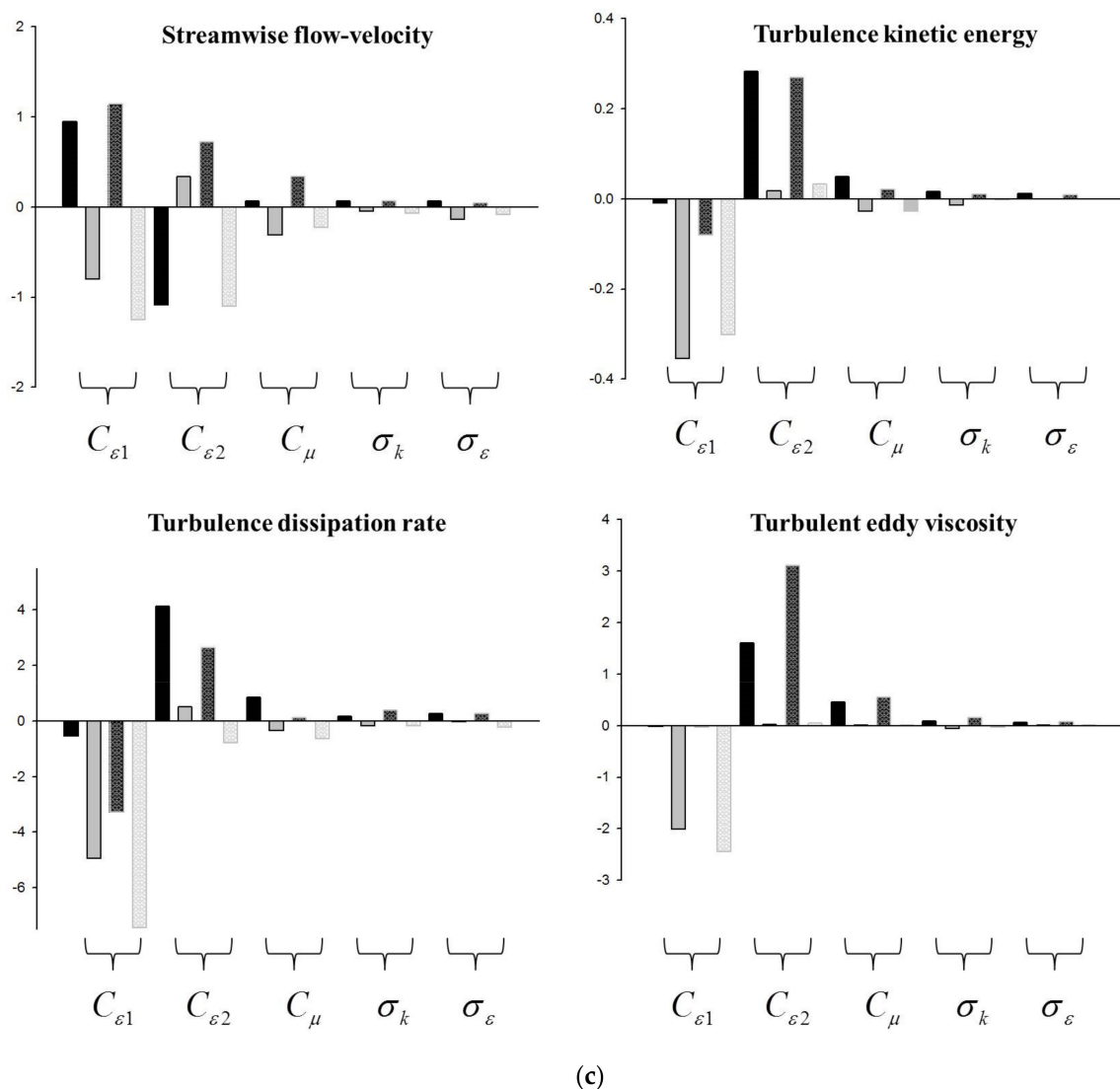
(**b**)

Figure 6. *Cont.*

Figure 6. Extreme value of the sensitivity coefficients with respect to the constants for the $k - \varepsilon$ turbulence model: (**a**) 20% opening, (**b**) 50% opening, (**c**) 80% opening case.

The notable observation in the sensitivity analysis was that the most sensitive flow property was the turbulence dissipation rate and this property was affected mainly by constants $C_{\varepsilon 1}$ and $C_{\varepsilon 2}$. Constants C_μ, σ_k and σ_ε hardly affected flow properties. Moreover, the constants affected flow properties differently depending on the disc opening percentage and locations. At the location of 5 x/Y, developing region, larger sensitivity values were observed with decreasing disc opening percentage. The sensitivity of flow properties was influenced mainly on the value of constant of $C_{\varepsilon 1}$. However, at the developed region of 10 x/Y, sensitivity value increased with increasing disc opening percentage. The sensitivity of flow properties was mainly influenced by constant, $C_{\varepsilon 2}$ except for 80% disc opening cases.

From the sensitivity analysis results for the $k - \varepsilon$ turbulence model, it was shown that sensitivity coefficients were mainly related with the flow behavior of the valve with different opening percentages. The sensitivity coefficient value increased with small opening case in the developing region, and with large opening in the developed region. From the result, the $k - \varepsilon$ turbulence model would be not suitable for the area of the large pressure drop and velocity increase. This is due to the relatively smaller effective flow region which resulted in a large pressure drop and velocity increase, leading to increasing turbulence.

5.2. Sensitivity Result of Two-Equation $k - \omega$ Model

For the $k - \omega$ turbulence model, the sensitivity coefficients of flow properties of stream-wise flow-velocity (u), turbulence kinetic energy (k), turbulence specific dissipation rate (ω), and turbulent eddy viscosity (μ_t) with regards to the constants were investigated. Figure 7 presents the extreme values of sensitivity coefficients with respect to the constants. The most sensitive flow property in this turbulence model was turbulence specific dissipation rate and this property was affected mainly by constant, β and partially by constant, α. The constants σ_k, σ_ω and β' hardly affected flow properties.

For the $k - \omega$ turbulence model, similar tendencies to the $k - \varepsilon$ turbulence model were observed: similar trends of individual sensitivity coefficients with disc opening and locations for the flow properties of stream-wise flow-velocity (u), turbulence kinetic energy (k), turbulent eddy viscosity (μ_t), except for the turbulence specific dissipation rate (ω). With regard to the sensitivity coefficient for the disc opening and the locations, decreasing sensitivity with increasing disc opening percentage at developing region of 5 x/Y, and increasing sensitivity with increasing disc opening percentage at developed region of 10 x/Y was observed. For the $k - \omega$ turbulence model, a relatively smaller value of sensitivity coefficient was observed. Moreover, difference of sensitivity coefficient with locations and opening were relatively smaller compared to the $k - \varepsilon$ turbulence model.

For the main two-equation of $k - \varepsilon$ and $k - \omega$ turbulence model, it can be suggested that turbulence constant adoptability in numerical calculations should be checked with respect to the flow characteristics when using each of the turbulence models. Especially for the case of the turbulence increasing area caused by large pressure drop and velocity increase, a test study of turbulence constant adoptability should be preceded.
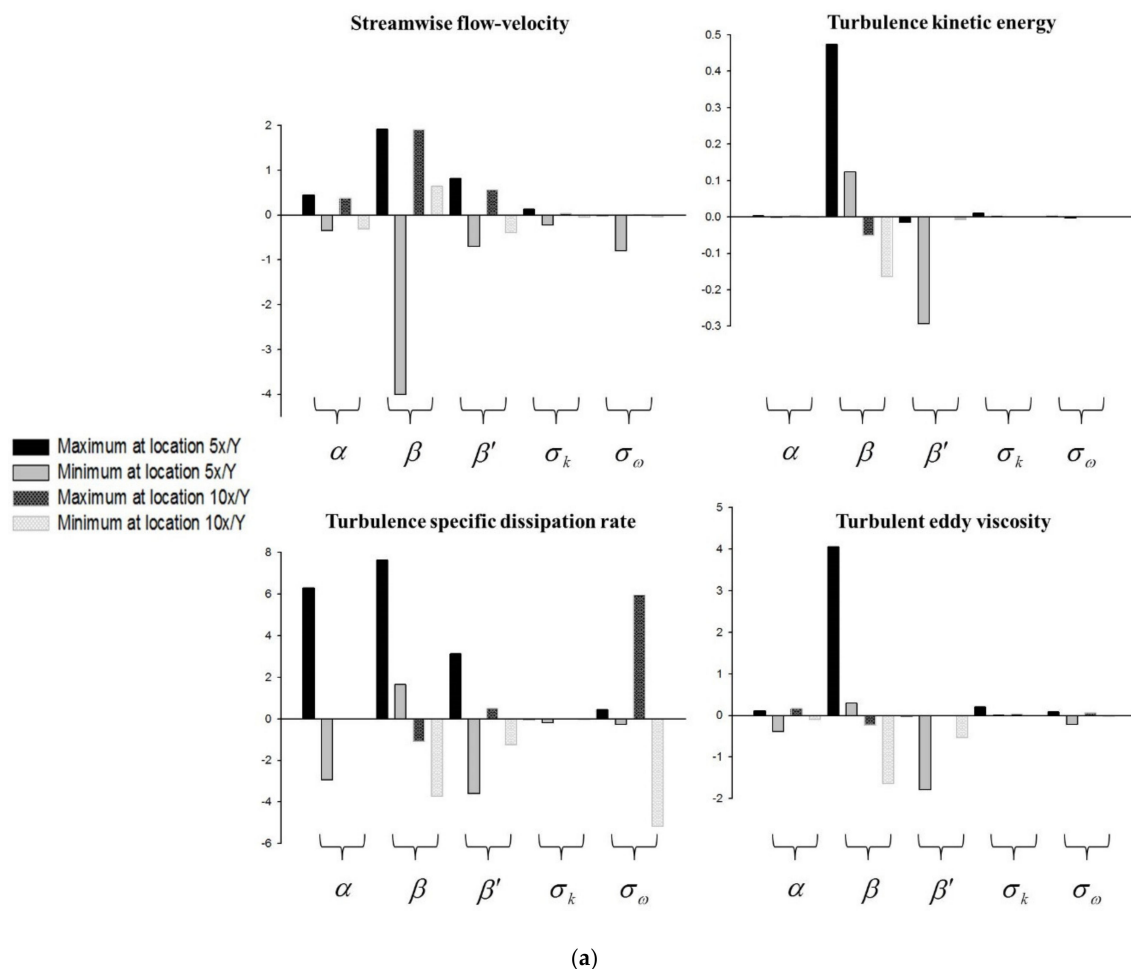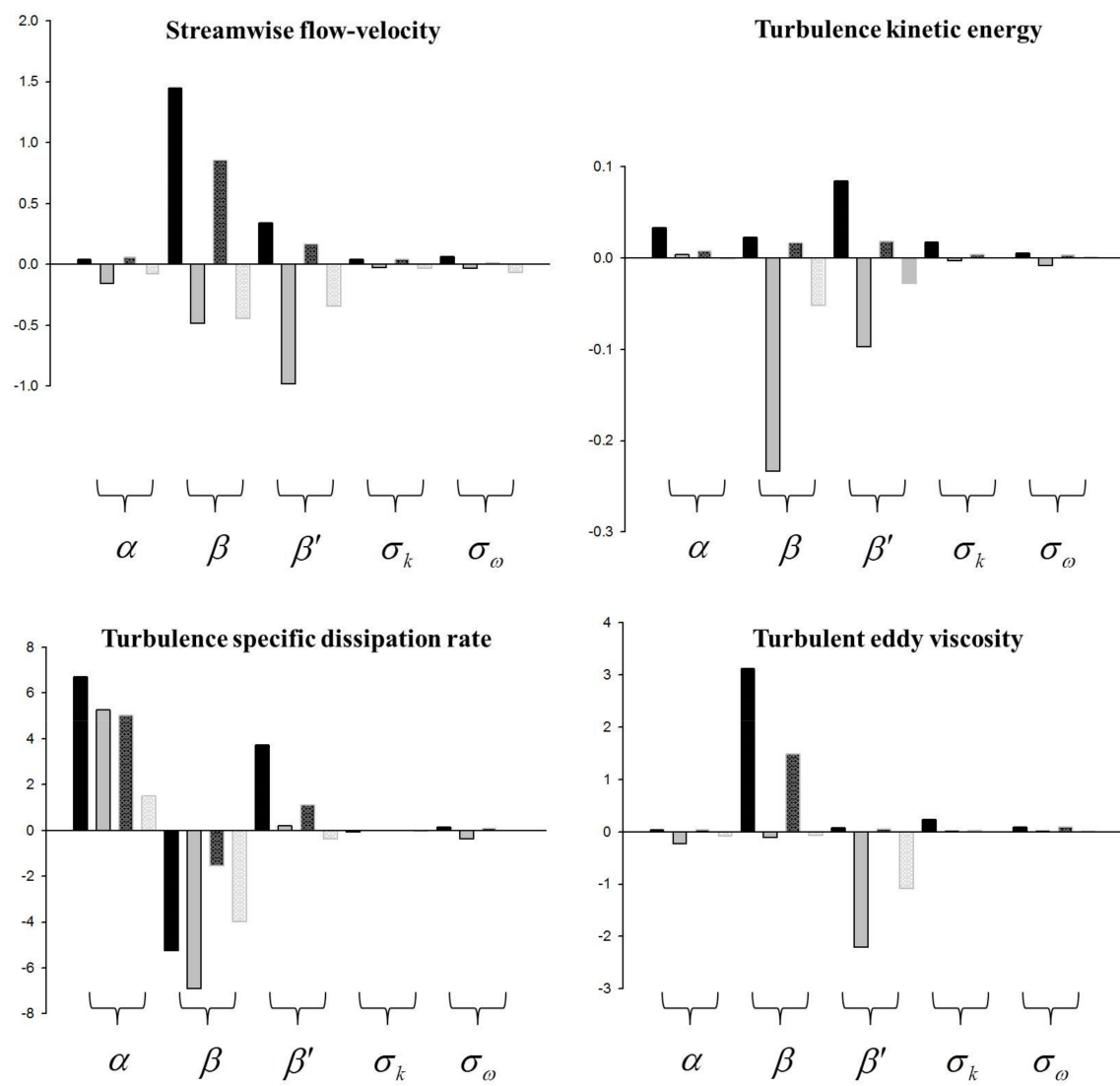

(a)

Figure 7. *Cont.*
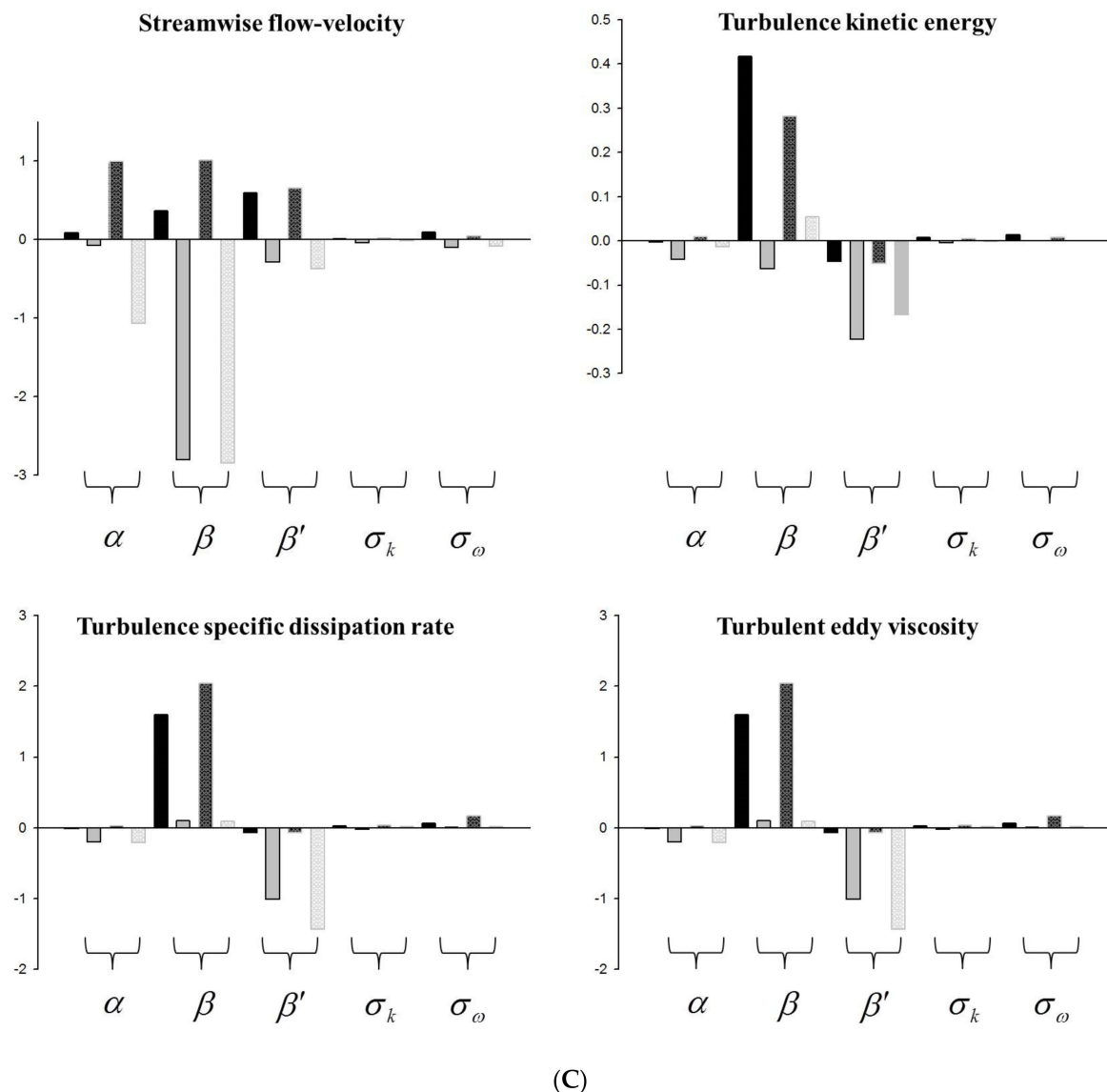
(**b**)

Figure 7. *Cont.*

(**C**)

Figure 7. Extreme value of the sensitivity coefficients with respect to the constants for the $k - \omega$ turbulence model: (**a**) 20% opening, (**b**) 50% opening, (**c**) 80% opening case.

6. Concluding Remarks

The flow behavior through a butterfly valve for three different-sized valves of DN 80 (76.2 mm), DN 262 (254 mm), and DN 400 (406 mm) was analyzed under various flow configurations and disc opening percentages. Two-equation $k - \varepsilon$, $k - \omega$, and SST turbulence models were assessed to determine the accuracy of numerical solutions and turbulence model effects on the valve flow coefficient were compared with experimental values. Sensitivity analysis of flow properties was conducted to determine the sensitivity of the constants used in the two-equation turbulence model. The main conclusions are as follows:

- With different-sized valves, discrepancies between numerical and experimental results for the flow coefficient were observed with different disc openings. The discrepancies increased with increasing valve size, and different degrees of discrepancy were observed with disc opening percentage for each valve size.
- Higher turbulence due to vortices was observed for the $k - \omega$ model expressed with higher turbulence kinetic energy, followed by the SST and $k - \varepsilon$ models. The difference between the results of turbulence models increased with decreasing valve size and disc opening. This can be attributed to the increasing turbulence effect which could

cause lots of discrepancies between turbulence models, especially in areas with large pressure drop and sharp velocity increase.

- The most sensitive flow property was turbulence dissipation rate and this property was mainly affected by the values of constants of $C_{\varepsilon 1}$ and $C_{\varepsilon 2}$ for the $k - \varepsilon$, $k - \omega$ turbulence model, and by the values of constants of β, partly by constant of α for the $k - \omega$ turbulence model.

- For the $k - \omega$ turbulence model, relatively smaller value of sensitivity with different locations and openings were observed compared to the $k - \varepsilon$ turbulence model. From sensitivity analysis results, it can be suggested that turbulence constant adoptability in numerical calculations should be checked when using each turbulence model.

- For the numerical calculations, currently three turbulence models were the most frequently used turbulent models. These models were advantageous over other turbulence models because the computational conditions could be easily implemented. Therefore, the investigated analysis will be helpful to current users of turbulence models. The results of this research could also be widely applied to engineering design using the various valve systems.

- The numerical approach presented in this paper can be effectively used in future research on various valve flow analyses especially for the cavitation phenomenon.

Author Contributions: Conceptualization, S.-W.C. and H.-S.K.; methodology, S.-W.C. and H.-S.K.; resources, H.-S.S.; data curation, H.-S.S.; writing—original draft preparation, S.-W.C.; writing—review and editing, S.-W.C. and H.-S.K.; visualization, H.-S.S.; supervision, S.-W.C. All authors have read and agreed to the published version of the manuscript. Authorship must be limited to those who have contributed substantially to the work reported.

Institutional Review Board Statement: Not applicable.

Informed Consent Statement: Not applicable.

Data Availability Statement: Not applicable.

Conflicts of Interest: The authors declare that they have no conflict of interest.

Nomenclature

a_d	Eddy viscosity constant
d	Wall distance
C_μ, $C_{1\omega}$, $C_{2\omega}$	Turbulence constant
CD_{kv}	Cross-diffusion in the $k - \omega$ model
C_v	Flow coefficient of the valve
F_1	Blending function
F_2	Auxiliary function
f_μ	Wall damping function
G_f	Specific gravity of the fluid
k	Turbulence kinetic energy
l	Turbulence mixing length
N_1	Constant in the valve flow coefficient
P	Turbulence production

Q	Flow rate
Re_t	Turbulence Reynolds number
S_{ij}	Mean velocity strain-rate tensor
$\widetilde{S}_m$	Sensitivity coefficient
t	Time
$\bar{u}$	Mean average velocity
u_s	Flow velocity parallel to the wall
w_1, w_2	Examined constants in sensitivity analysis
y_+	Wall function
x/Y	Specific location (x: distance from the valve, Y; nominal valve size)
y/Y	Specific location (y: height, Y; nominal valve size)
ΔC_m	Increment of turbulence constant
Δp	Pressure drop across the valve
Greek Symbols	
τ_{ij}	Turbulence Reynolds stress
δ_{ij}	Kronecker delta tensor
μ	Dynamic viscosity
μ_t	Turbulence eddy viscosity
ε	Turbulence dissipation rate
ω	Specific turbulent dissipation rate
Ω	Vorticity
ρ	Density of the material
γ	Ratio of specific heat
$\varphi_k, \varphi_\varepsilon$	Explicit wall term
α, α'	Turbulence constant
β, β'	Turbulence constant
$\sigma_k, \sigma_\varepsilon, \sigma_\omega$	Turbulence constant

References

1. Kaartinen, N.H.; Juhala, P.J. Fluid Flow Control Device. U.S. Patent No. 4,258,740, 31 March 1981.
2. Smith, P.; Zappe, R.W. *Valve Selection Handbook: Engineering Fundamentals for Selecting the Right Valve Design for Every Industrial Flow Application*; Elsevier: Amsterdam, The Netherlands, 2004.
3. American Water Works Association. *Problem Organisms in Water*; American Water Works Association: Denver, CO, USA, 2004.
4. Del Toro, A.; Johnson, M.C.; Spall, R.E. Computational fluid dynamics investigation of butterfly valve performance factors. *J. Am. Water Work. Assoc.* **2015**, *107*, E243–E254. [CrossRef]
5. Lin, F.; Schohl, G. CFD Prediction and Validation of Butterfly Valve Hydrodynamic Forces. In *Critical Transitions in Water and Environmental Resources Management*; American Society of Civil Engineers: Reston, VA, USA, 2004; pp. 1–8.
6. Song, X.; Wang, L.; Park, Y. Fluid and Structural Analysis of Large Butterfly Valve. In *AIP Conference Proceedings*; American Institute of Physics: College Park, MD, USA, 2008; pp. 311–314.
7. Guan Song, X.; Park, Y. Numerical Analysis of Butterfly Valve-Prediction of Flow Coefficient and Hydrodynamic Torque Coefficient. In Proceedings of the World Congress on Engineering and Computer Science, San Francisco, CA, USA, 24–26 October 2007; pp. 24–26.
8. Henderson, A.D.; Sargison, J.E.; Walker, G.J.; Haynes, J. A numerical prediction of the hydrodynamic torque acting on a safety butterfly valve in a hydro-electric power scheme. *WSEAS Trans. Fluid Mech.* **2008**, *1*, 218.
9. Huang, C.; Kim, R. Three-dimensional analysis of partially open butterfly valve flows. *J. Fluids Eng.* **1996**, *118*, 562–568. [CrossRef]
10. Blevins, R. *Applied Fluid Dynamics Handbook*; Van Nostrand Reinhold Co.: New York, NY, USA, 1984.
11. Davis, J.; Stewart, M. Predicting globe control valve performance—Part I: CFD modeling. *J. Fluids Eng.* **2002**, *124*, 772–777. [CrossRef]
12. Chern, M.; Wang, C. Control of volumetric flow-rate of ball valve using V-port. *J. Fluids Eng.* **2004**, *126*, 471–481. [CrossRef]
13. Hinz, D.; Kim, T.; Fried, E. Statistics of the Navier–Stokes-alpha-beta regularization model for fluid turbulence. *J. Phys. A Math. Theor.* **2014**, *47*, 055501. [CrossRef]
14. Thalabard, S.; Nazarenko, S.; Galtier, S.; Medvedev, S. Anomalous spectral laws in differential models of turbulence. *J. Phys. A Math. Theor.* **2015**, *48*, 285501. [CrossRef]
15. Rigola, J.; Aljure, D.; Lehmkuhl, O.; Perez-Segarra, C.D.; Oliva, A. Numerical Analysis of the Turbulent Fluid Flow Through Valves. Geometrical Aspects Influence at Different Positions. In *IOP Conference Series: Materials Science and Engineering*; IOP Publishing: Bristol, UK, 2015; p. 012026.
16. Zhang, S.C.; Zhang, Y.L.; Fang, Z.M. Numerical simulation and analysis of ball valve three-dimensional flow based on CFD. In *IOP Conference Series: Earth and Environmental Science*; IOP Publishing: Bristol, UK, 2012; p. 052024.

17. Leutwyler, Z.; Dalton, C. A computational study of torque and forces due to compressible flow on a butterfly valve disk in mid-stroke position. *J. Fluids Eng.* **2006**, *128*, 1074–1082. [CrossRef]
18. Said, M.M.; Abdelmeguid, H.; Rabie, L. The Accuracy Degree of CFD Turbulence Models for Butterfly Valve Flow Coefficient Prediction. *Am. J. Ind. Eng.* **2016**, *4*, 14–20.
19. Wu, X.; Wallace, J.; Hickey, J. Boundary layer turbulence and freestream turbulence interface, turbulent spot and freestream turbulence interface, laminar boundary layer and freestream turbulence interface. *Phys. Fluids* **2019**, *31*, 045104. [CrossRef]
20. Sharma, M.; Verma, M.; Chakraborty, S. Anisotropic energy transfers in rapidly rotating turbulence. *Phys. Fluids* **2019**, *31*, 085117. [CrossRef]
21. Li, H.; Yang, Z. Separated boundary layer transition under pressure gradient in the presence of free-stream turbulence. *Phys. Fluids* **2019**, *31*, 104106.
22. Wilcox, D. Comparison of two-equation turbulence models for boundary layers with pressure gradient. *AIAA J.* **1993**, *31*, 1414–1421. [CrossRef]
23. Wilcox, D. *Turbulence Modeling for CFD*; DCW industries: La Canada, CA, USA, 1998.
24. Jones, W.P.; Launder, B. The prediction of laminarization with a two-equation model of turbulence. *Int. J. Heat Mass Transf.* **1972**, *15*, 301–314. [CrossRef]
25. Launder, B.; Sharma, B. Application of the energy-dissipation model of turbulence to the calculation of flow near a spinning disc. *Lett. Heat Mass Transf.* **1974**, *1*, 131–137. [CrossRef]
26. Pletcher, R.; Tannehill, J.; Anderson, D. *Computational Fluid Mechanics and Heat Transfer*; CRC Press: Boca Raton, FL, USA, 2012.
27. Bottema, M. Turbulence closure model constants and the problems of inactive atmospheric turbulence. *J. Wind. Eng. Ind. Aerodyn.* **1997**, *67*, 897–908. [CrossRef]
28. Comte-Bellot, G.; Corrsin, S. The use of a contraction to improve the isotropy of grid-generated turbulence. *J. Fluid Mech.* **1966**, *25*, 657–682. [CrossRef]
29. Hrenya, C.M.; Bolio, E.J.; Chakrabarti, D.; Sinclair, J.L. Comparison of low Reynolds number $k - \varepsilon$ turbulence models in predicting fully developed pipe flow. *Chem. Eng. Sci.* **1995**, *50*, 1923–1941. [CrossRef]
30. Launder, B.; Spalding, D. The numerical computation of turbulent flows. In Numerical prediction of flow, heat transfer, turbulence and combustion. *Pergamon* **1983**, 96–116. [CrossRef]
31. Launder, B.E.; Spalding, D.B. *Lectures in Mathematical Models of Turbulence*; Academic Press: New York, NY, USA, 1972.
32. Shih, T.H. An improved k-epsilon model for near-wall turbulence and comparison with direct numerical simulation. *NASA STI Recon Tech. Rep. N* **1990**, *90*, 27983.
33. Sarkar, A.; So, R.M.C. A critical evaluation of near-wall two-equation models against direct numerical simulation data. *Int. J. Heat Fluid. Flow.* **1997**, *18*, 197–208. [CrossRef]
34. Chen, Y.-S.; Kim, S.-W. *Computation of Turbulent Flows Using an Extended k-Epsilon Turbulence Closure Model*; NASA CR-179204; Universities Space Research Association: Columbia, MD, USA; Science and Engineering Directorate: Ottawa, ON, Canada, 1987.
35. Sarkar, T.; Sayer, P.G.; Fraser, S.M. Flow simulation past axisymmetric bodies using four different turbulence models. *Appl. Math. Model.* **1997**, *21*, 783–792. [CrossRef]
36. Shih, T.-H.; Liou, W.W.; Shabbir, A.; Yang, Z.; Zhu, J. A new k-ε eddy viscosity model for high reynolds number turbulent flows. *Comput. Fluids* **1995**, *24*, 227–238. [CrossRef]
37. Błazik-Borowa, E. The analysis of the channel flow sensitivity to the parameters of the k–ε method. *Int. J. Numer. Methods Fluids* **2008**, *58*, 1257–1286. [CrossRef]
38. Benton, J.; Kalitzin, G.; Gould, A. Application of two-equation turbulence models in aircraft design. In Proceedings of the 34th Aerospace Sciences Meeting and Exhibit, Reno, NV, USA, 15–18 January 1996; p. 327.
39. Wilcox, D.C. Formulation of the kw turbulence model revisited. *AIAA J.* **2008**, *46*, 2823–2838. [CrossRef]
40. Huang, P.G.; Bardina, J.; Coakley, T. Turbulence modeling validation, testing, and development. *NASA Tech. Memo.* **1997**, *110446*, 147.
41. Kok, J.C. Resolving the dependence on freestream values for the k-turbulence model. *AIAA J.* **2000**, *38*, 1292–1295. [CrossRef]
42. Kim, M.-S.; Ryu, J.-H.; Oh, S.-J.; Yang, J.-H.; Choi, S.-W. Numerical Investigation on Influence of Gas and Turbulence Model for Type III Hydrogen Tank under Discharge Condition. *Energies* **2020**, *13*, 6432. [CrossRef]
43. Menter, F.; Ferreira, J.C.; Esch, T.; Konno, B. The SST Turbulence Model with Improved Wall Treatment for Heat Transfer Predictions in Gas Turbines. In Proceedings of the International Gas Turbine Congress, Tokyo, Japan, 2–7 November 2003.
44. Williams, S.; Trembley, J.; Miller, J.P. Flow Monitoring using Flow Control Device. U.S. Patent No. 7,092,797, 15 August 2006.
45. ISA. *Standard, Control Valve Sizing Equations for Compressible Fluids, ISA-S75*; The International Society of Automation: Research Triangle Park, NC, USA, 2007.
46. ISA. *Standard, Control Valve Capacity Test Procedures, ISA-S75*; The International Society of Automation: Research Triangle Park, NC, USA, 2007.
47. Hutchison, J. *ISA Handbook of Control Valves: A Comprehensive Reference Book Containing Application and Design Information*; Instrument Society of America: Research Triangle Park, NC, USA, 1976.
48. Sandalci, M.; Mancuhan, E.; Alpman, E.; Kucukada, K. Effect of the flow conditions and valve size on butterfly valve performance. *J. Therm. Sci. Technol.* **2010**, *3*, 103–112.

49. Nazary, H.; Aalipour, N.; Alizadeh, M. Investigation of the Flow and Cavitation in a Butterfly Calve. *J. Mech. Res. Appl.* **2011**, *3*, 37–47.
50. Kim, C.K.; Yoon, J.Y.; Shin, M.S. Experimental study for flow characteristics and performance evaluation of butterfly valves. In *IOP Conference Series: Earth and Environmental Science*; IOP Publishing: Bristol, UK, 2010; p. 012098.
51. ANSYS, Inc. *ANSYS CFX-Solver Modeling Guide*; Release 12.0; ANSYS, Inc.: Canonsburg, PA, USA, 2009; Volume 15, pp. 162–168.
52. Blocken, B.; Gualtieri, C. Ten iterative steps for model development and evaluation applied to Computational Fluid Dynamics for Environmental Fluid Mechanics. *Environ. Model. Softw.* **2012**, *33*, 1–22. [CrossRef]
53. Patel, Y. Numerical Investigation of Flow Past a Circular Cylinder and in a Staggered Tube Bundle Using Various Turbulence Models. Master's Thesis, Lappeenranta University of Technology, Faculty of Technology, Lappeenranta, Finland, 24 August 2010.
54. Błazik-Borowa, E. The application example of the sensitivity analysis of the solution to coefficients of the k-ε model. *Budownictwo i Architektura* **2012**, *10*, 53–68. [CrossRef]
55. Colin, E.; Etienne, S.; Pelletier, D.; Borggaard, J. Application of a sensitivity equation method to turbulent flows with heat transfer. *Int. J. Therm. Sci.* **2005**, *44*, 1024–1038. [CrossRef]